Supplemental material

O'Shaughnessy et al., https://doi.org/10.1083/jcb.201903019

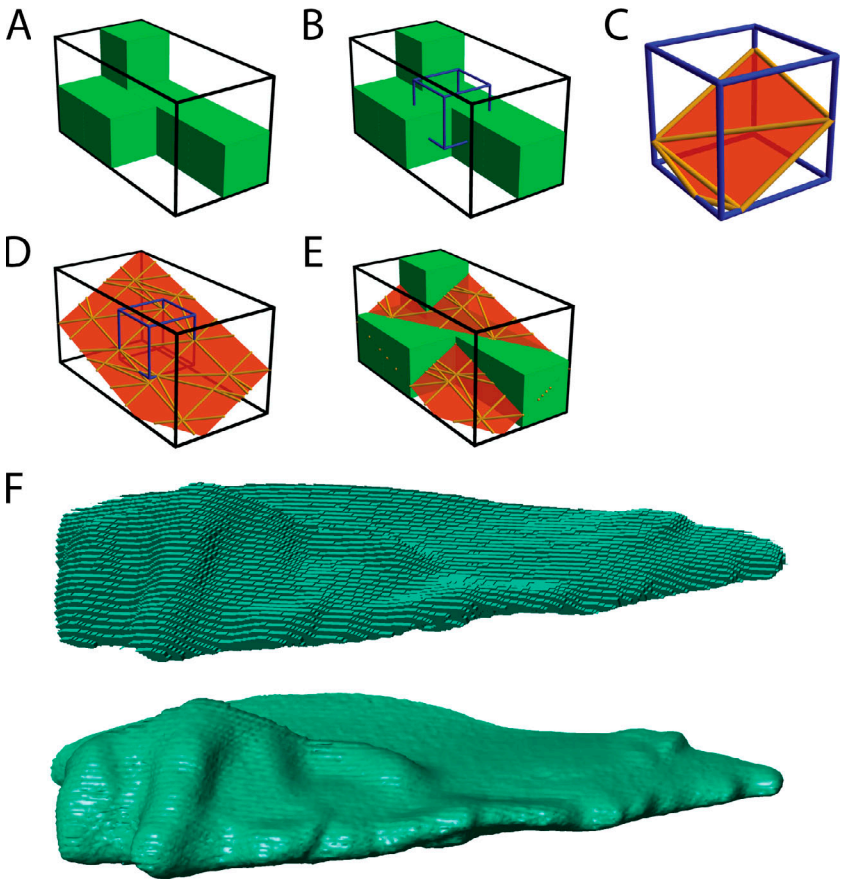

Figure S1. **Tessellation via the marching cubes algorithm on a 3D grid.** A step-by-step representation of the marching cubes algorithm to render a surface. **(A)** Cubes within the 3D grid (black outline) are marked as either in the object (green cubes) or not. **(B)** A data cell (blue outline) is drawn with vertices at the centers of the neighboring cubes. **(C)** Using linear interpolation along all three axes, vertices for triangular faces (red face, yellow outline) are evaluated along the edges of the data cell. This generates the tessellated surface within that region of the 3D grid. **(D)** Each data cell is evaluated to generate a fully connected surface across the entire 3D grid. **(E)** The tessellated surface rendered via the marching cubes algorithm represents a much more physical surface than the original pixelated object. **(F)** A visual comparison between 3D surface renderings of a region of actual cell data.

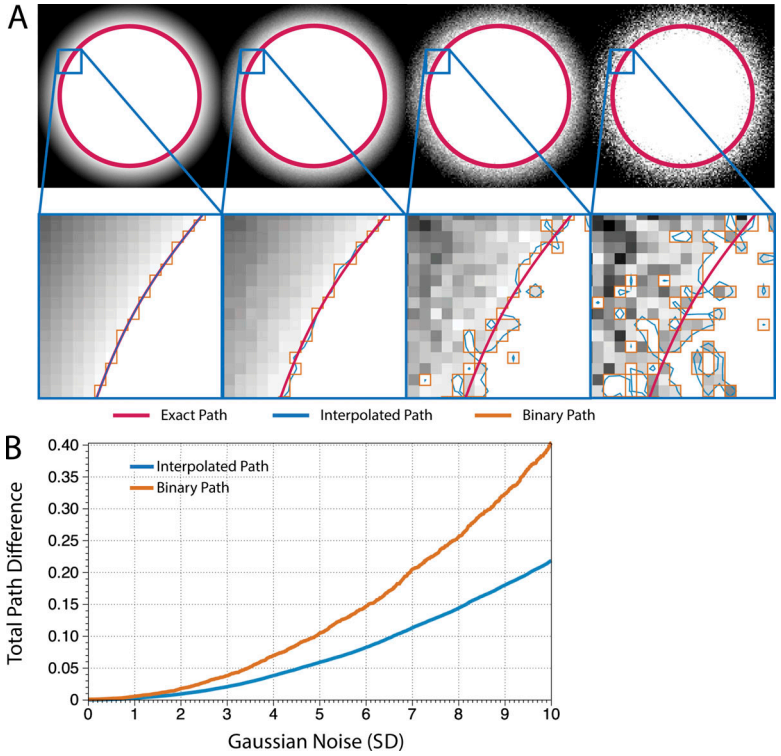

Figure S2. **Interpolation produces a more accurate representation of a surface than a binary mask.** For simplicity, illustrations are shown in 2D, but the approach applies to 3D as well. **(A)** An idealized circle (pink) is blurred with increasing levels of Gaussian noise (SDs of 0.0, 0.35, 2.0, and 5.0). Two methods to segment the edge are shown: interpolation (blue) and a binary, pixel-based method (orange). Bilinear interpolation uses local data at each pixel vertex to approximate the boundary at a subpixel level. **(B)** To quantify the deviation between each calculated path and the exact boundary, the shortest line segment from every vertex to the exact boundary was determined. The sum (integral) of these line segments was calculated over a range of Gaussian noise levels.

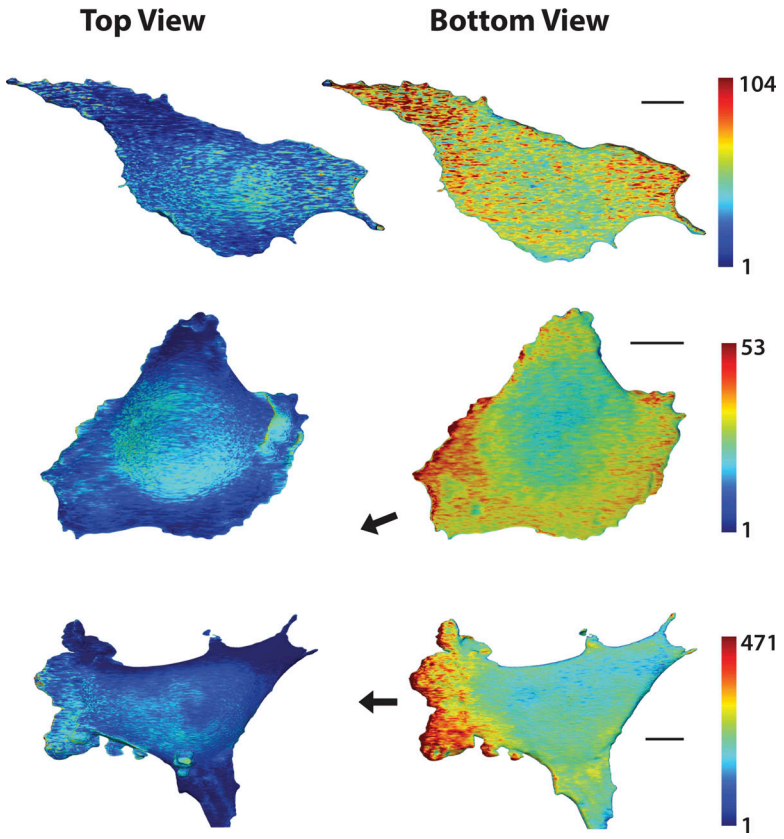

Figure S3. **Comparison of Rap1 activity on the dorsal and ventral surfaces.** Rap1 activity is consistently higher on the ventral (bottom) surface of the Cos7 cells and shows broad regions of high activity. Color scale indicates corrected FRET/CFP, excluding the highest and lowest 2% of ratio values to eliminate spurious pixels. Scale bars, 10 µm. Note that we show scale bars for the bottom of the cell, which is relatively flat, with minimal perspective.

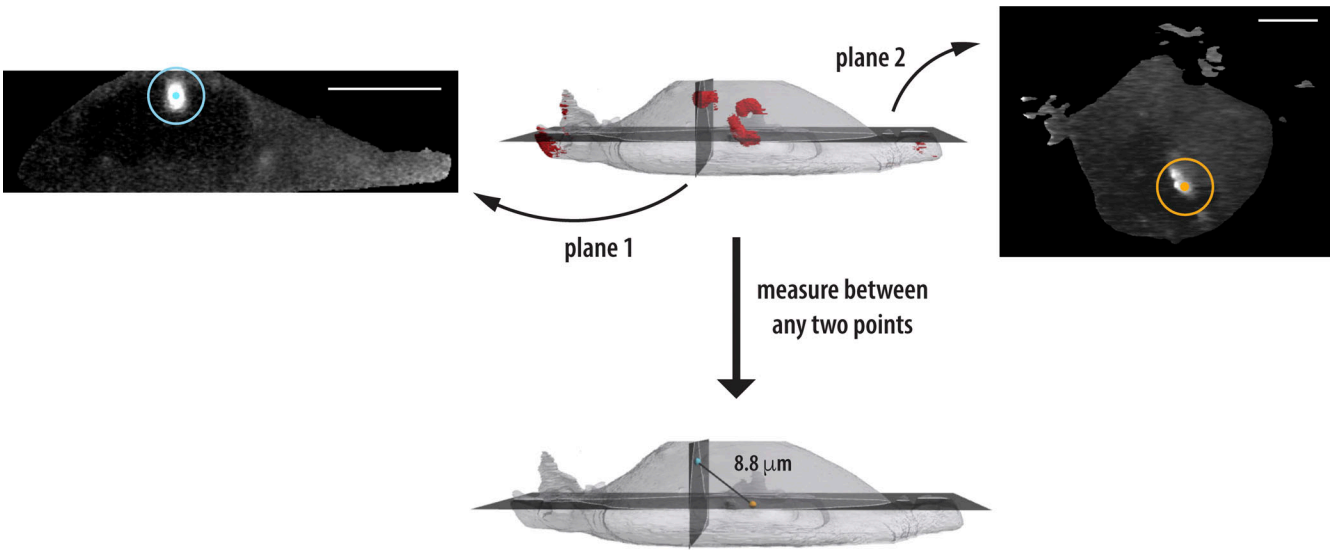

Figure S4. **Measurement tool.** This tool measures the distance between any two points in the cell. Two independent planes can be moved to any location in the cell (the planes can be horizontal, vertical, or rotated), and a point on each plane is selected. Scale bars on each plane are 10 µm. A line is fit between the points, and its length is returned in micrometers.

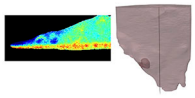

Video 1. **Vesicle emerging from the ventral cell membrane.**

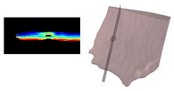

Video 2. **Vesicle fusing with the ventral cell membrane.**

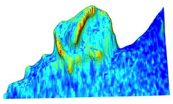

Video 3. **Rap1 activation within ruffle.**

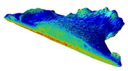

Video 4. **Rap1 activation within ruffle.**

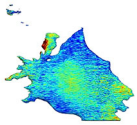

Video 5. **High Rap1 activity in protrusions viewed from the bottom of the cell.**

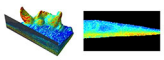

Video 6. **Moving cross-section of a ruffle at a single time point.** Note that the activity underlying the ruffle extends at some points to the ventral surface.

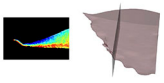

Video 7. **Vesicle formed by a folding ruffle.**

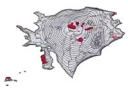

Video 8. **Internal regions of high activity rotate counter-clockwise.**